Cross-Subject Assistance: Inter- and Intra-Subject Maximal Correlation for Enhancing the Performance of SSVEP-Based BCIs

Haoran Wang, Yaoru Sun, Fang Wang, Lei Cao, Wei Zhou, Zijian Wang, Shiyi Chen

***Abstract*— *Objective:* The current state-of-the-art methods significantly improve the detection performance of the steady-state visual evoked potentials (SSVEPs) by using the individual calibration data. However, the time-consuming calibration sessions limit the number of training trials and may give rise to visual fatigue, which weakens the effectiveness of the individual training data. For addressing this issue, this study proposes a novel inter- and intra-subject maximal correlation (IISMC) method to enhance the robustness of SSVEP recognition via employing the inter- and intra-subject similarity and variability. Through efficient transfer learning, similar experience under the same task is shared across subjects. *Methods:* IISMC extracts subject-specific information and similar task-related information from oneself and other subjects performing the same task by maximizing the inter- and intra-subject correlation. Multiple weak classifiers are built from several existing subjects and then integrated to construct the strong classifiers by the average weighting. Finally, a powerful fusion predictor is obtained for target recognition. *Results:* The proposed framework is validated on a benchmark data set of 35 subjects, and the experimental results demonstrate that IISMC obtains better performance than the state of the art task-related component analysis (TRCA). *Significance:* The proposed method has great potential for developing high-speed BCIs.**

***Index Terms*— Brain computer interface (BCI), electroencephalography (EEG), steady-state visual evoked potentials (SSVEP), inter- and intra-subject maximal correlation, transfer learning.**

I. Introduction

BRAIN-COMPUTER interfaces (BCIs) based on steady-state visual evoked potentials (SSVEPs) have been investigated extensively due to high signal-to-noise ratio (SNR), high information transfer rate (ITR), reliability, and design flexibility [1]–[3]. In a recent study, researchers proposed a new joint frequency-phase modulation (JFPM) method to tag 40 characters in an SSVEP-based BCI speller, resulting in achieving an ITR of 267 bits/min on average, the highest ITR to date [3]. In the literature, the JFPM paradigm incorporated phase coding into frequency coding, which could minimize the correlation coefficient between adjacent frequency stimuli. Besides, the SSVEP template signals obtained by averaging across multiple trials in the calibration data for each stimulus class were used to improve the classification performance of demodulation paradigm.

Previous studies for SSVEP recognition focused on the amplitude and spatial distribution of SSVEP responses, such as power spectral density analysis (PSDA), where the frequency corresponding to the peak value is taken as the visual stimulus frequency. However, only the single-channel EEG data is used, the PSDA is sensitive to background noises and requires a long time window for improving recognition accuracy [4]. In recent years, many spatial filtering techniques based on multiple channel signals have been introduced to implement more efficient SSVEP-based BCIs, such as canonical correlation analysis (CCA) [5], minimum energy combination (MEC) [6] and multivariate synchronization index (MSI) [7]. Among them, the CCA has been most widely adopted and robust enough in detecting SSVEPs.

Although the standard CCA is highly efficient for the frequency detection of SSVEPs, the recognition accuracy is not satisfactory because the simplified pre-constructed sine-cosine waves are almost devoid of the abundant features contained in the real EEG data. Currently, researchers have been trying to extract the subject-specific and task-related information from the individual calibration data and reduce the effect of spontaneous background EEG activities. The individual template-based CCA (IT-CCA) [8] method was recently proposed to replace the sine-cosine reference signals with individual template signals. Alternatively, another way is to optimize the reference signals, such as the multi-way CCA (MwayCCA) [9], the L1-regularized MwayCCA (L1-MCCA) [4] and the multi-set CCA (MsetCCA) [10]. It has been proved that these calibration-data-based methods significantly outperform the standard CCA method. In general, the individualized template signals can better characterize subject-specific SSVEPs, compared to the optimized reference signals. The combined CCA (Combined-CCA) incorporating individual templates into the CCA leads to a higher performance than the other existing CCA-based methods [11]. Recent state-of-the-art SSVEP decoders learn spatial filters from the calibration data via maximizing the inter-trial correlations, then calculate the

This work was supported by the National Natural Science Foundation of China (91748122).

H. Wang, Y. Sun, Z. Wang and S. Chen are with the Department of Computer Science and Technology, Tongji University, Shanghai 201804, China. Corresponding author: Yaoru Sun (e-mail: yaoru@tongji.edu.cn).

F. Wang is with the Department of Computer Science, Brunel University, Uxbridge UB8 3PH, U.K.

L. Cao is with the Department of Computer Science and Technology, School of Information and Engineering, Shanghai Maritime University, Shanghai 201306, China.

W. Zhou is with the Department of Information and Communication Engineering, Tongji University, Shanghai 201804, China.

correlation between the test data and transformed individual templates, such as the task-related component analysis (TRCA) [12], the correlated component analysis (CORCA) [13] and the sum of squared correlations (SSCOR) [14].

Previous studies depend on the assumption that task-related information is stable and similar across trials, which means that sufficient amounts of training data are required for extracting essential features [3]. However, the time-consuming and labor-intensive training procedure will hinder the practical application of an SSVEP-based BCI speller. For addressing the issue, subject-independent training methods, which require the training data from various subjects to extract common features or generalize system parameters so that the BCI application is suitable for a new user, have drawn the attention of researchers [15]. Subject-independent training methods adopt the cross-subject transfer-learning to provide inter-subject similarity, e.g., transfer template-based canonical correlation analysis (tt-CCA), online transfer template-based CCA (ott-CCA) [16], transfer template-based Combined-CCA (Combined-tCCA) and a unsupervised adaptive transfer variant of Combined-tCCA (Adaptive-C3A) [17]. These methods establish transferred templates by averaging the training data across all source subjects, and the transferred templates are regarded as the alternative to individual templates. A recent study extends the TRCA by maximizing reproducible components across trials and a group of subjects, referred to as group TRCA (gTRCA) [18]. The gTRCA exploits the similarity between a new subject and the existing subjects for recognizing stimuli, which offers an alternative to grand averaging.

Although subject-independent training methods have outperformed training-free methods, they are not comparable to subject-dependent training methods requiring the individual data to extract subject-specific information. For this reason, the session-to-session transfer method has been proposed, which transfers training data of the same subjects recorded from different days [19]. Another recent study proposes least-squares transformation (LST) that transforms the training data from several existing subjects to fit individual data and form a supplement to individual data [20]. When the number of individual trials is limited, the LST can significantly enhance the SSVEP decoding performance. In fact, inherent intra-subject variability may impede the inter-trial transferability. For example, visual fatigue and attention lapse often result in varying amplitude of response, latency, and SSVEP attend-to-ignore ratios (AIR) [21]–[24]. The inter-subject associativity, based on transferring knowledge, can alleviate intra-subject variability and reduce the necessity for calibration sessions [25].

This study proposed a cross-subject assistance framework to enhance the robustness of SSVEP recognition by maximizing inter- and intra-subject correlation. Not only subject-specific information but also, more importantly, the inter-subject similarity is integrated into the method, and thus further can improve the separability of the extracted features. In the performance evaluation, the efficacy of the proposed framework was evaluated on a 40-target SSVEP dataset recorded from 35 subjects [26]. The results in this paper demonstrated that the proposed method significantly enhanced the recognition performance and outperformed the state of the art TRCA, especially in the case of less training data.

II. Materials and Methods

A. Benchmark Dataset

The proposed framework was evaluated using the SSVEP benchmark data provided by Wang et al. [26]. The dataset was recorded from 35 healthy subjects (17 females, aged 17–34 years, mean age: 22 years). Among these subjects, eight of them had experience of using the SSVEP-based BCI speller, and others were naive to the SSVEP-based BCI. The user interface of the BCI speller is a 5×8 stimulus matrix containing 40 characters (26 English alphabet letters, 10 digits, and 4 other symbols). The 40 characters are coded using linearly increasing frequencies and phases. The frequency range is from 8 Hz to 15.8 Hz with an interval of 0.2 Hz. The phase values start from 0, and the interval is 0.5 π.

For each subject, the experiment consisted of six runs, each containing 40 trials corresponding to all 40 characters. Each trial started with a 0.5-s target cue, which prompted users to shift their gaze to the target as soon as possible. After that, all stimuli started to flicker on the monitor concurrently for 5 s. After the stimulus was rendered, there was a rest for 0.5 s to avoid visual fatigue. The EEG data were collected from 64 electrodes positioned according to the international extended 10-20 system, and the reference electrode was placed at the vertex (Cz).

In the evaluation process, the EEG data was selected from 9 electrodes ($\mathrm{O_Z}$, $\mathrm{O_1}$, $\mathrm{O_2}$, $\mathrm{P_Z}$, $\mathrm{PO_Z}$, $\mathrm{PO_3}$, $\mathrm{PO_4}$, $\mathrm{PO_5}$ and $\mathrm{PO_Z}$) and was extracted in [0.14 s (0.14 +d) s], where d is the data length used in the analysis. The delay of 0.14 s was applied to suppress the effect of visual latencies in the visual system [27]. All data epochs were downsampled to 250 Hz and then were filtered via a band-pass IIR filter to pass signals between 7 Hz and 90 Hz.

B. Task Related Component Analysis

Task related component analysis (TRCA) was employed to extract task-related components by maximizing the inter-trial covariances [12]. Assume that $\boldsymbol{X}_i \in \mathbb{R}^{N_c \times N_s}$ and $\boldsymbol{X}_j \in \mathbb{R}^{N_c \times N_s}$ are the i-th and j-th trial of one subject. Here, N_c is the number of channels, N_s is the number of time samples. The constrained optimization is given by the Rayleigh-Ritz problem [14]:

$$\boldsymbol{w} = \arg\max_{\boldsymbol{w}} \frac{\boldsymbol{w}^T \boldsymbol{S} \boldsymbol{w}}{\boldsymbol{w}^T \boldsymbol{Q} \boldsymbol{w}} \tag{1}$$

Here, $\boldsymbol{S}$ is the aggregated inter-trial covariances:

$$\boldsymbol{S} = \sum_{\substack{i,j=1 \\ i \neq j}}^{N_t} Cov(\boldsymbol{X}_i, \boldsymbol{X}_j) \tag{2}$$

$\boldsymbol{Q}$ is the aggregated auto-covariances:

$$\boldsymbol{Q} = \sum_{\substack{i,j=1 \\ i = j}}^{N_t} Cov(\boldsymbol{X}_i, \boldsymbol{X}_j) \tag{3}$$

where N_t is the number of training trials. The optimal coefficient vector $\boldsymbol{w}$ can be obtained as the eigenvector of the matrix $\boldsymbol{Q}^{-1}\boldsymbol{S}$ corresponding to the largest eigenvalue. Then, $\boldsymbol{w}_k$, the spatial filter for the k-th stimulus frequency, can be obtained. The correlation coefficients r_k (i.e., the feature λ_k for target identification) between projections of test trial $\boldsymbol{X}_t \in \mathbb{R}^{N_c \times N_s}$ and the averaged training data across trials $\bar{\boldsymbol{X}}_k \in \mathbb{R}^{N_c \times N_s}$ can be calculated as follow:

$$\lambda_k = r_k = \rho(\boldsymbol{X}_t^T \boldsymbol{w}_k, \bar{\boldsymbol{X}}_k^T \boldsymbol{w}_k) \tag{4}$$

where $\rho(a, b)$ indicates the correlation coefficient between a and b. After that, the target frequency f_t can be recognized by the formula:

$$f_t = \max_{f_k} \lambda_k, k = 1, \ldots, N_f \tag{5}$$

where N_f is the number of stimuli used in SSVEP-based BCI.

C. Inter- and Intra-Subject Maximal Correlation (IISMC)

This study focuses on extracting subject-specific information and similar task-related information from oneself and other subjects performing the same task, that are inspired by the TRCA and CORCA.

1) Inter-subject maximal correlation: Assume that EEG signals of the i-th and j-th trial recorded from the subject S_1 and S_2 are denoted as $\boldsymbol{X}_{S_1,i} \in \mathbb{R}^{N_c \times N_s}$ and $\boldsymbol{X}_{S_2,j} \in \mathbb{R}^{N_c \times N_s}$, respectively. And N_{t1} and N_{t2} are the numbers of training trials. The objective of inter-subject maximal correlation is to find a linear combination (i.e., spatial filter) of electrodes that maximize the correlation between subjects [28]. Formally, such a weight vector $\boldsymbol{w}$ is sought that the resulting linear projections $\boldsymbol{y}_{S_1,i} = \boldsymbol{w}^T \boldsymbol{X}_{S_1,i}$ and $\boldsymbol{y}_{S_2,j} = \boldsymbol{w}^T \boldsymbol{X}_{S_2,j}$ exhibit the maximal Pearson Product Moment Correlation Coefficient [29]. Therefore the optimization problem can be solved as:

$$\boldsymbol{w} = \arg\max_{\boldsymbol{w}} \frac{1}{2} \frac{\boldsymbol{w}^T(\boldsymbol{R}_{12} + \boldsymbol{R}_{21})\boldsymbol{w}}{\sqrt{\boldsymbol{w}^T \boldsymbol{R}_{11} \boldsymbol{w}} \sqrt{\boldsymbol{w}^T \boldsymbol{R}_{22} \boldsymbol{w}}} \tag{6}$$

Here, $\boldsymbol{R}_{12}$ and $\boldsymbol{R}_{21}$ are the inter-subject cross-covariances:

$$\boldsymbol{R}_{12} = \frac{1}{N_{t1} N_{t2}} \sum_{i=1}^{N_{t1}} \sum_{j=1}^{N_{t2}} (\boldsymbol{y}_{S_1,i} - \overline{\boldsymbol{y}}_{S_1,i})(\boldsymbol{y}_{S_2,j} - \overline{\boldsymbol{y}}_{S_2,j})^T \tag{7}$$

$$\boldsymbol{R}_{21} = \frac{1}{N_{t1} N_{t2}} \sum_{i=1}^{N_{t1}} \sum_{j=1}^{N_{t2}} (\boldsymbol{y}_{S_2,j} - \overline{\boldsymbol{y}}_{S_2,j})(\boldsymbol{y}_{S_1,i} - \overline{\boldsymbol{y}}_{S_1,i})^T \tag{8}$$

$\boldsymbol{R}_{11}$ and $\boldsymbol{R}_{22}$ are the intra-subject auto-covariances:

$$\boldsymbol{R}_{11} = \frac{1}{N_{t1}} \sum_{i=1}^{N_{t1}} (\boldsymbol{y}_{S_1,i} - \overline{\boldsymbol{y}}_{S_1,i})(\boldsymbol{y}_{S_1,i} - \overline{\boldsymbol{y}}_{S_1,i})^T \tag{9}$$

$$\boldsymbol{R}_{22} = \frac{1}{N_{t2}} \sum_{j=1}^{N_{t2}} (\boldsymbol{y}_{S_2,j} - \overline{\boldsymbol{y}}_{S_2,j})(\boldsymbol{y}_{S_2,j} - \overline{\boldsymbol{y}}_{S_2,j})^T \tag{10}$$

Assume that $\boldsymbol{w}^T \boldsymbol{R}_{11} \boldsymbol{w}$ and $\boldsymbol{w}^T \boldsymbol{R}_{22} \boldsymbol{w}$ are equal [13], [30], [31], which yields the following equation:

$$\sqrt{\boldsymbol{w}^T \boldsymbol{R}_{11} \boldsymbol{w}} \sqrt{\boldsymbol{w}^T \boldsymbol{R}_{22} \boldsymbol{w}} = \frac{1}{2} \boldsymbol{w}^T (\boldsymbol{R}_{11} + \boldsymbol{R}_{22}) \boldsymbol{w} \tag{11}$$

Hence the equation (6) can be simplified to:

$$\boldsymbol{w} = \arg\max_{\boldsymbol{w}} \frac{\boldsymbol{w}^T(\boldsymbol{R}_{12} + \boldsymbol{R}_{21})\boldsymbol{w}}{\boldsymbol{w}^T(\boldsymbol{R}_{11} + \boldsymbol{R}_{22})\boldsymbol{w}} \tag{12}$$

The optimal weight vector $\boldsymbol{w}$ can be obtained from the eigenvector of $(\boldsymbol{R}_{11} + \boldsymbol{R}_{22})^{-1}(\boldsymbol{R}_{12} + \boldsymbol{R}_{21})$, which is corresponding to the largest eigenvalue.

2) Intra-subject maximal correlation: Assume that $\boldsymbol{X}_i \in \mathbb{R}^{N_c \times N_s}$ and $\boldsymbol{X}_j \in \mathbb{R}^{N_c \times N_s}$ are the i-th and j-th trial of the same subject. Same as above, a weight vector $\check{\boldsymbol{w}}$ is sought so that the resulting linear projections $\boldsymbol{y}_i = \check{\boldsymbol{w}}^T \boldsymbol{X}_i$ and $\boldsymbol{y}_j = \check{\boldsymbol{w}}^T \boldsymbol{X}_j$ exhibit the maximal Pearson's correlation. Hence the optimization problem can be solved as:

$$\check{\boldsymbol{w}} = \arg\max_{\check{\boldsymbol{w}}} \frac{1}{2} \frac{\check{\boldsymbol{w}}^T(\check{\boldsymbol{R}}_{12} + \check{\boldsymbol{R}}_{21})\check{\boldsymbol{w}}}{\sqrt{\check{\boldsymbol{w}}^T \check{\boldsymbol{R}}_{11} \check{\boldsymbol{w}}} \sqrt{\check{\boldsymbol{w}}^T \check{\boldsymbol{R}}_{22} \check{\boldsymbol{w}}}} \tag{13}$$

Here, $\check{\boldsymbol{R}}_{12}$ and $\check{\boldsymbol{R}}_{21}$ are the within-subject cross-covariances:

$$\check{\boldsymbol{R}}_{12} = \frac{2}{N_t(N_t - 1)} \sum_{i<j \le N_t} (\boldsymbol{y}_i - \overline{\boldsymbol{y}}_i)(\boldsymbol{y}_j - \overline{\boldsymbol{y}}_j)^T \tag{14}$$

$$\check{\boldsymbol{R}}_{21} = \frac{2}{N_t(N_t - 1)} \sum_{i<j \le N_t} (\boldsymbol{y}_j - \overline{\boldsymbol{y}}_j)(\boldsymbol{y}_i - \overline{\boldsymbol{y}}_i)^T \tag{15}$$

where N_t is the number of training trials belonged to the subject. $\check{\boldsymbol{R}}_{11}$ and $\check{\boldsymbol{R}}_{22}$ are the within-subject auto-covariances:

$$\check{\boldsymbol{R}}_{11} = \check{\boldsymbol{R}}_{22} = \frac{1}{N_t} \sum_{i=j \le N_t} (\boldsymbol{y}_i - \overline{\boldsymbol{y}}_i)(\boldsymbol{y}_j - \overline{\boldsymbol{y}}_j)^T \tag{16}$$

In the same way, the equation (13) can be simplified to:

$$\check{\boldsymbol{w}} = \arg\max_{\check{\boldsymbol{w}}} \frac{\check{\boldsymbol{w}}^T(\check{\boldsymbol{R}}_{12} + \check{\boldsymbol{R}}_{21})\check{\boldsymbol{w}}}{\check{\boldsymbol{w}}^T(\check{\boldsymbol{R}}_{11} + \check{\boldsymbol{R}}_{22})\check{\boldsymbol{w}}} \tag{17}$$

Similarly, $\check{\boldsymbol{w}}$ can be obtained from the eigenvector of $(\check{\boldsymbol{R}}_{11} + \check{\boldsymbol{R}}_{22})^{-1}(\check{\boldsymbol{R}}_{12} + \check{\boldsymbol{R}}_{21})$, which is corresponding to the largest eigenvalue.

3) Combined inter- and intra-subject maximal correlation: Suppose S_M is the set of selected subjects used for transfer, while S_I is the current individual whose test trials will be recognized. For the k-th stimulus frequency f_k, the template signals of the transferred subjects are obtained by averaging training trials:

$$\bar{\boldsymbol{X}}_{S_m,k} = \frac{1}{N_{tm}} \sum_{i=1}^{N_{tm}} \boldsymbol{X}_{S_m,k,i}, \forall S_m \in S_M \tag{18}$$

where $\boldsymbol{X}_{S_m,k,i}$ is the i-th trial of the subject S_m corresponding to f_k, and N_{tm} is the number of training trials. The individual template signals are obtained as follow:

$$\bar{\boldsymbol{X}}_k = \frac{1}{N_t} \sum_{i=1}^{N_t} \boldsymbol{X}_{k,i} \tag{19}$$

where $\boldsymbol{X}_{k,i}$ is the i-th trial of the current individual corresponding to f_k, and N_t is the number of individual training trials. Then the inter-subject spatial filters $\{\boldsymbol{w}_{S_m,k}|S_m \in S_M\}$ between each pair $\{(S_m, S_I)|S_m \in S_M\}$ of transferred subject S_m and individual S_I can be obtained via inter-subject maximal correlation, i.e., the equation (12). The intra-subject spatial filter $\check{\boldsymbol{w}}_k$ can be obtained via intra-subject maximal correlation, i.e., the equation (17).

By incorporating these template signals and spatial filters in target identification, four different types of correlation coefficients between projections of test trial $\boldsymbol{X}_t$ and template signals are implemented as follows: (i) $\rho(\boldsymbol{X}_t^T\check{\boldsymbol{w}}_k, \bar{\boldsymbol{X}}_k^T\check{\boldsymbol{w}}_k)$ with individual template and intra-subject spatial filter, (ii) $\rho(\boldsymbol{X}_t^T\boldsymbol{w}_{S_m,k}, \bar{\boldsymbol{X}}_k^T\boldsymbol{w}_{S_m,k})$ with individual template and inter-subject spatial filter, (iii) $\rho(\boldsymbol{X}_t^T\check{\boldsymbol{w}}_k, \bar{\boldsymbol{X}}_{S_m,k}^T\check{\boldsymbol{w}}_k)$ with transferred subject's template and intra-subject spatial filter, (iiii) $\rho(\boldsymbol{X}_t^T\boldsymbol{w}_{S_m,k}, \bar{\boldsymbol{X}}_{S_m,k}^T\boldsymbol{w}_{S_m,k})$ with transferred subject's template and inter-subject spatial filter.

In essence, for each transferred subject, (ii), (iii) and (iiii) can be obtained, and they are all weak classifiers. Strong classifiers can be constructed by averaging their "votes" of weak classifiers [32], [33]. Hence, for the k-th stimulus frequency, a correlation vector $\boldsymbol{r}_k$ is defined as follows:

$$\begin{aligned}\boldsymbol{r}_k &= \begin{bmatrix} r_k(1) \\ r_k(2) \\ r_k(3) \\ r_k(4) \end{bmatrix} \\ &= \begin{bmatrix} \rho(\boldsymbol{X}_t^T\check{\boldsymbol{w}}_k, \bar{\boldsymbol{X}}_k^T\check{\boldsymbol{w}}_k) \\ \frac{1}{|S_M|}\sum_{S_m\in S_M}\rho(\boldsymbol{X}_t^T\boldsymbol{w}_{S_m,k}, \bar{\boldsymbol{X}}_k^T\boldsymbol{w}_{S_m,k}) \\ \frac{1}{|S_M|}\sum_{S_m\in S_M}\rho(\boldsymbol{X}_t^T\check{\boldsymbol{w}}_k, \bar{\boldsymbol{X}}_{S_m,k}^T\check{\boldsymbol{w}}_k) \\ \frac{1}{|S_M|}\sum_{S_m\in S_M}\rho(\boldsymbol{X}_t^T\boldsymbol{w}_{S_m,k}, \bar{\boldsymbol{X}}_{S_m,k}^T\boldsymbol{w}_{S_m,k}) \end{bmatrix}\end{aligned} \tag{20}$$

where $\sum_{S_m\in S_M}$ represents the sum over all transferred subjects. In the end, the four correlation values described in equation (20) are combined as the feature for target identification:

$$\lambda_k = \sum_{n=1}^{4} sign(r_k(n)) \cdot (r_k(n))^2 \tag{21}$$

where $sign()$ is used to keep discriminative information from negative correlation coefficients. Then, the target frequency f_t can be recognized by the formula (5). Fig. 1 illustrates the proposed IISMC-based method.

D. The Ensemble Strategy

For each subject, previous studies have demonstrated that these spatial filters $\{\boldsymbol{w}_1^*, \ldots, \boldsymbol{w}_{N_f}^*\}$ obtained from different stimuli are similar to each other because distributed local sources of the SSVEP response are similar [34]. Combining these spatial filters can further improve the performance of methods [12]–[14]. The ensemble spatial filter is given as:

$$\boldsymbol{W} = [\boldsymbol{w}_1^*, \ldots, \boldsymbol{w}_{N_f}^*] \tag{22}$$

Then the correlation coefficient for k-th visual stimulus between a test data $\boldsymbol{X}_t$ and the relevant template signal $\boldsymbol{Y}_k$ can be modified to be as:

$$r_k^* = \rho(\boldsymbol{X}_t^T\boldsymbol{W}^T, \boldsymbol{Y}_k^T\boldsymbol{W}^T) \tag{23}$$

Hereinafter, the ensemble TRCA-based and IISMC-based methods were termed as e-TRCA and e-IISMC, respectively.

E. Filter-Bank Processing

The filter-bank technology decomposes SSVEPs into sub-band components, and then extracts the high-SNR independent information embedded in the harmonic components. Hence the filter-bank technology can facilitate target classification [35]. In this study, the lower and upper cut-off frequencies were set to $b\times 8$ Hz and 90 Hz for the b-th sub-band, where the range of b is from 1 to N_b. After that, the feature $\lambda_k^{(b)}$ was extracted from the b-th sub-band signals filtered by Chebyshev Type I Infinite impulse response (IIR). A weighted sum of squares of feature values from all sub-bands is obtained as the final detection score:

$$\Lambda_k = \sum_{b=1}^{N_b} v(b)(\lambda_k^{(b)})^2 \tag{24}$$

where $v(b) = b^{(-1.25)} + 0.25$ is the weight function. And the target frequency f_t can be recognized by the formula:

$$f_t = \max_{f_k} \Lambda_k, k = 1, \ldots, N_f \tag{25}$$

F. Performance Evaluation

The accuracy (%) and ITR (bit/min) comparisons between the proposed IISMC-based methods and the state-of-the-art TRCA-based methods were performed. The classification accuracy was estimated using a leave-one-out cross-validation, i.e., 5 blocks were used for training, and 1 block was used for testing. In the IISMC-based methods, for each transferred subject, all 6 blocks were used.

It is worth noting that the experienced group was reported that it had a higher CCA classification accuracy [26], which means that they could provide more useful task-related information. Thus the IISMC-based methods based on two subject groups (i.e., the experienced group and all 35 subjects) were investigated, respectively. The former, termed as IISMC-EG, randomly selected partial individuals from 8 experienced subjects. The latter, termed as IISMC, was the general version and randomly selected subjects from all 35 subjects. For statistical significance, each random process was repeated 10 times and the averaged results were reported.

To evaluate the discriminative ability and the similarity of features extracted with the IISMC-based and the TRCA-based methods, the t-Distributed Stochastic Neighbor Embedding (t-SNE) technique was employed to map original data in high dimensions onto low dimensions [36]. Specifically, the t-SNE establishes joint probabilities of data points based on similarity and tries to minimize the Kullback-Leibler divergence between

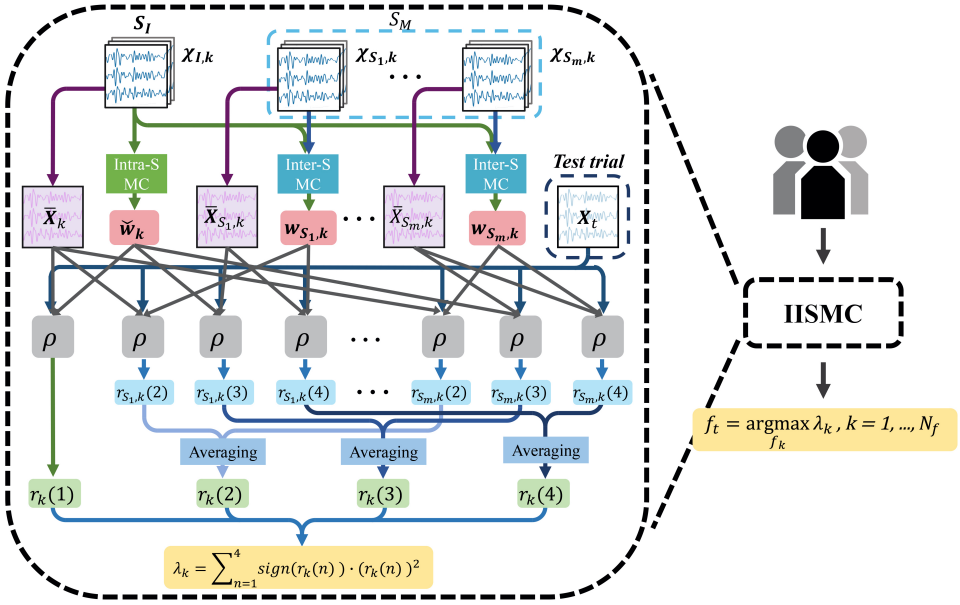

Fig. 1: Flowchart of the IISMC-based method for SSVEP frequency recognition. $\boldsymbol{\chi}_{I,k}$ denotes the individual training data at the k-th stimulus frequency $f_k (k = 1, \ldots, N_f)$, and $\boldsymbol{\chi}_{S_1,k}, \ldots, \boldsymbol{\chi}_{S_m,k}$ denote the training data recorded from transferred subjects $S_1, \ldots, S_m$. Then the spatial filters (e.g., $\tilde{\boldsymbol{w}}_k$, $\boldsymbol{w}_{S_1,k}$, and $\boldsymbol{w}_{S_m,k}$) can be found by the inter-subject maximal correlation (Inter-S MC) and the intra-subject maximal correlation (Intra-S MC), and four different type of correlation coefficients between projections of the test trial X_t and various template signals (e.g., $\bar{\boldsymbol{X}}_k$, $\bar{\boldsymbol{X}}_{S_1,k}$, and $\bar{\boldsymbol{X}}_{S_m,k}$) are calculated by the Pearson's correlation ρ. These correlation coefficients are integrated by the the formula (20). The SSVEP frequency for X_t is finally recognized by formula (21).

the joint probabilities of the low-dimensional and the high-dimensional data. In this study, the t-SNE algorithm mapped 40-dimensional features extracted with the IISMC-based and the TRCA-based methods to a 2-dimensional vector so that the extracted features were visualized in two dimensions. The data visualization technique would provide a more intuitive interpretation and insightful implication of the experimental findings. Meanwhile, for quantifying the degree of (intra-cluster) compactness and (inter-cluster) separation of cluster partitions formed by these 2-dimensional points, the mean silhouette coefficient over all 40 clusters was calculated. The larger value of silhouette coefficient indicates that data points within the same cluster are more closely aggregated, and the distance between adjacent clusters is more longer [37], [38]. In this study, the distance between points was calculated by the Euclidean distance.

III. Results

A. Parameter Optimization

1) Transferred Subject Selection: Since the number of subjects used for transfer $|S_M|$ would play an important role in the IISMC method, we first explored the effects of varying $|S_M|$ on the recognition performance. Fig. 2 showed the averaged classification accuracy for the basic and ensemble versions of the IISMC method using 600-ms long SSVEP data, where the $|S_M|$ varied from 1 to 7. Clearly, the IISMC-EG outperformed the general IISMC, indicating that the known experienced subjects who had a few training and experience of using the SSVEP-based BCI speller would provide better guidance for other subjects' target identification. When the number of transferred subjects was more than 2, these IISMC-based methods yielded better performance compared to the TRCA-based methods. Overall, the accuracy obtained by the IISMC-based methods increased with the number of transferred subjects used in the calculation. However, the statistically significant difference between adjacent values of $|S_M|$ was very small when the number of transferred subjects was more than 4. As a result, the setting $|S_M| = 5$ was adopted for further analysis, which was also the resource-accuracy trade-off.

2) Filter-Bank Analysis: For the 600-ms data length, the classification performances of the TRCA and IISMC with different number of sub-bands were compared. As shown in Fig. 3, the IISMC-based methods achieved higher accuracy than the TRCA-based methods in all cases. Furthermore, the highest accuracy was obtained when the numbers of sub-bands were 4 and 5 for the basic and ensemble versions of IISMC-based and TRCA-based methods, which is consistent with the result reported in the literature [3], [12]–[14]. For a fair comparison, in the following computation, the number of sub-bands was set to 4.

B. Target Identification Performance

1) Training Blocks: An important objective of the IISMC method is to reduce the dependency on the individual calibration data. It means that the proposed method can be sensitive enough to detect SSVEPs with adequate accuracy as the number of individual training blocks is reduced. Fig. 4 showed the average accuracies of the IISMC-based and TRCA-based

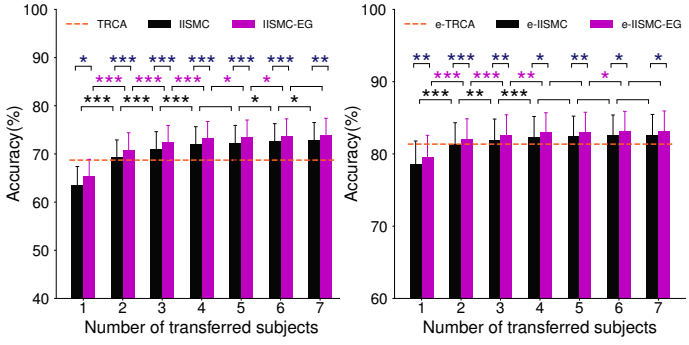

(a) (b)

Fig. 2: The averaged classification accuracy obtained by (a) the basic and (b) the ensemble version of IISMC-based methods at different numbers of transferred subjects with 600ms-long epochs. The dash line indicates the baseline (i.e., the accuracy of TRCA). The asterisk indicates the statistically significant differences (paired t-tests, $*p < 0.05$; $**p < 0.01$; $***p < 0.001$). The error bars indicate standard errors.

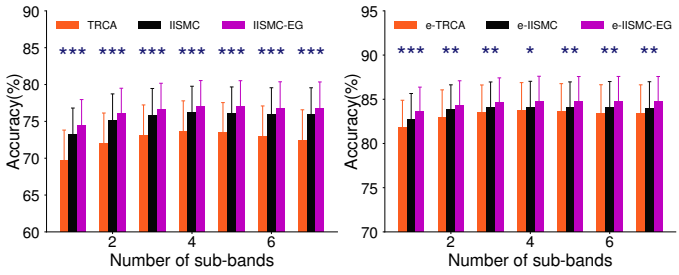

(a) (b)

Fig. 3: The averaged classification accuracy obtained by (a) the basic and (b) the ensemble versions of IISMC-based and TRCA-based methods at different numbers of sub-bands with 600ms-long epochs. The error bars indicate standard errors. The asterisk indicates significant difference between three methods by one-way repeated measures analysis of variance (ANOVA) ($*p < 0.05$; $**p < 0.01$; $***p < 0.001$).

methods for different number of individual training blocks at a 600-ms time window. For the IISMC-based methods, the stacked bars were plotted for different numbers of transferred subjects' training blocks, and darker colors represented lower numbers. Overall, the classification accuracy increased with the number of training blocks, and the IISMC-based methods outperformed the TRCA-based methods. In particular, when the number of training blocks for both the individual and other transferred subjects was 2, the IISMC-based methods dramatically improved the detection accuracy (TRCA versus IISMC versus IISMC-EG without filter bank: $40.79 \pm 4.46\%$ versus $47.40 \pm 4.29\%$ versus $49.18 \pm 4.22\%$; TRCA versus IISMC versus IISMC-EG with filter bank: $43.29 \pm 4.59\%$ versus $49.22 \pm 4.41\%$ versus $50.87 \pm 4.33\%$; e-TRCA versus e-IISMC versus e-IISMC-EG without filter bank: $60.89 \pm 4.74\%$ versus $62.68 \pm 4.54\%$ versus $64.32 \pm 4.42\%$; e-TRCA versus e-IISMC versus e-IISMC-EG with filter bank: $62.18 \pm 4.90\%$ versus $64.06 \pm 4.48\%$ versus $65.84 \pm 4.29\%$). With the increasing numbers of the individual calibration data, the promotion was weakened, but the performance of IISMC was still slightly better than the TRCA and did not deteriorate to the same level.

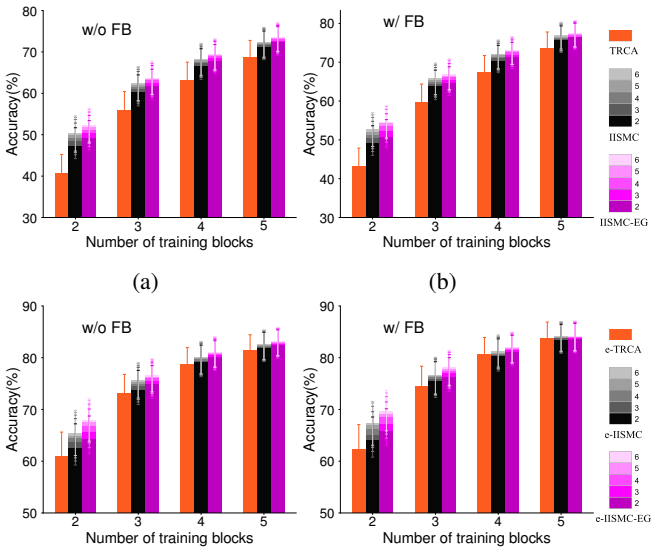

(a) (b) (c) (d)

Fig. 4: The performance comparison between IISMC and TRCA for different number of individual training blocks with 600ms-long epochs. The stacked bars represent the number of training blocks from the transferred subject, in which darker colors mean less amount. The subplots (a) and (b) show the mean accuracy of the basic methods while subplots (c) and (d) show the ensemble methods. The first and second columns depict the results of these methods without and with the filter-bank (w/o FB and w/ FB) technology, respectively. The error bars indicate standard errors.

2) Overall Performance: The average accuracies for the IISMC-based and the TRCA-based methods were compared at different time lengths (0.2-1 s). These results were presented in Fig. 5. The IISMC-based methods yielded better performance than the TRCA-based methods in case of both the basic and the ensemble versions. By the statistical analysis with paired t-tests, the proposed IISMC-based methods showed superiority compared to the TRCA-based methods when the time window was greater than 0.2 s. Furthermore, the IISMC-EG method showed a significant improvement regardless of the time-window length.

The performance of the proposed IISMC method using the filter bank was further investigated. As shown in Fig. 6, for the basic version, the IISMC-based methods outperformed the TRCA-based methods in all situations. However, the classification accuracies of the ensemble IISMC method based on the randomized group were nearly similar to those of the ensemble TRCA method, with no statistically significant difference between them via paired t-tests. But, as expected, the ensemble IISMC method based on the experienced group still had an apparent performance improvement compared with the ensemble TRCA method. The differences were obvious and statistically significant.

The difference between results obtained by the IISMC and

This article has been accepted for publication in a future issue of this journal, but has not been fully edited. Content may change prior to final publication. Citation information: DOI 10.1109/TNSRE.2021.3057938, IEEE Transactions on Neural Systems and Rehabilitation Engineering

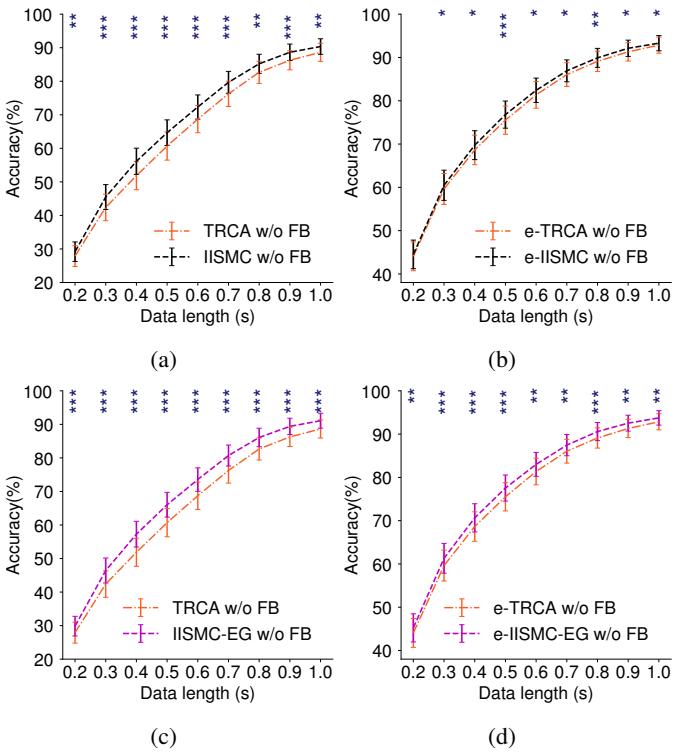

Fig. 5: The average accuracies across all subjects obtained by the IISMC-based methods and the TRCA-based methods at different data length without filter-bank (w/o FB) preprocessing. The first and second rows depict the results obtained by the IISMC method based on the randomized group and the experienced group, respectively. The asterisk indicates the statistically significant differences (paired t-tests, $*p < 0.05$; $**p < 0.01$; $***p < 0.001$). The error bars indicate standard errors.

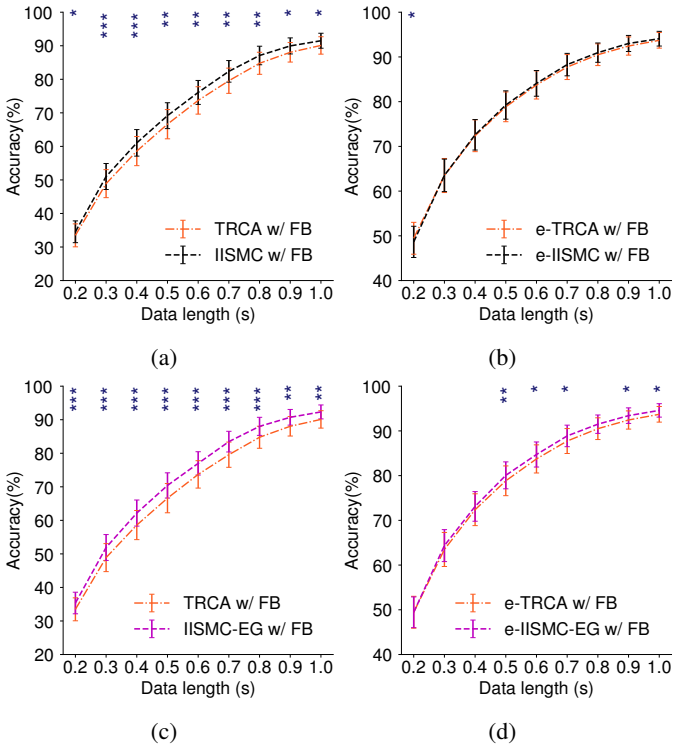

Fig. 6: The average accuracies across all subjects obtained by the IISMC-based methods and the TRCA-based methods at different data length with filter-bank (w/ FB) preprocessing. The first and second rows depict the results obtained by the IISMC method based on the randomized group and the experienced group, respectively. The asterisk indicates the statistically significant differences (paired t-tests, $*p < 0.05$; $**p < 0.01$; $***p < 0.001$). The error bars indicate standard errors.

the IISMC-EG was caused by different groups of transferred source subjects, which encouraged us to divide all subjects into three groups (i.e., 8 experienced, 27 naive, and all 35 subjects) and further investigate the accuracy of three groups. Figure. 7 illustrated the average accuracies of three groups. The window was set to 0.6 s, by the statistical analysis with paired t-tests, there was no statistically significant difference for the experienced group between the IISMC-based and the TRCA-based methods at all conditions. However, there still was a statistically significant difference for the naive group, which was basically conformable to the result of all 35 subjects. It demonstrated that the proposed method could significantly enhance accuracy of the inexperienced subject but have little impact on the experienced subject who usually have high accuracy. On the contrary, the reliable experience of the experienced group was obviously of great importance for the IISMC method, which applied shared experience to a target subject. For this reason, the accuracies and ITRs of the ensemble IISMC methods based on the experienced group were compared with those results from the ensemble TRCA methods. As shown in Fig. 8, the ensemble IISMC method with filter-bank preprocessing achieved the highest ITR (e-IISMC w/ FB: 219.66 $\pm$ 10.20 bits/min, t = 0.5 s; e-TRCA w/ FB: 217.02 $\pm$ 11.06 bits/min, t = 0.6 s; e-IISMC w/o FB: 211.3 $\pm$ 8.61 bits/min, t = 0.6 s; e-TRCA w/o FB: 206.68 $\pm$ 9.32 bits/min, t = 0.7 s). These findings suggested that inter-subject shared information can indeed significantly enhance the recognition of SSVEPs.

C. The t-SNE Visualization

This study exploited the fundamental assumption of evoked responses: reproducibility of task-related components across trials and subjects [39]. The IISMC not only utilized subject-specific information but also, more importantly, explicitly integrated the inter-subject similarity into the model, thus further improving the separability of features for different stimulus classes. To further investigate the discriminative ability and the similarity of features extracted by these compared methods, the 2-dimensional t-SNE of the 40-dimensional features was implemented and visualized in Fig. 9. Fig. 9 illustrated the t-SNE projections of the feature vectors from the IISMC-based and the TRCA-based methods for an example subject (S22). Obviously, these two-dimensional points obtained by the IISMC-based methods were more tightly aggregated within the clusters, and these formed clusters were well-separated, when compared with the TRCA-based methods. These observations were quantified using the silhouette coefficient: 0.322 for

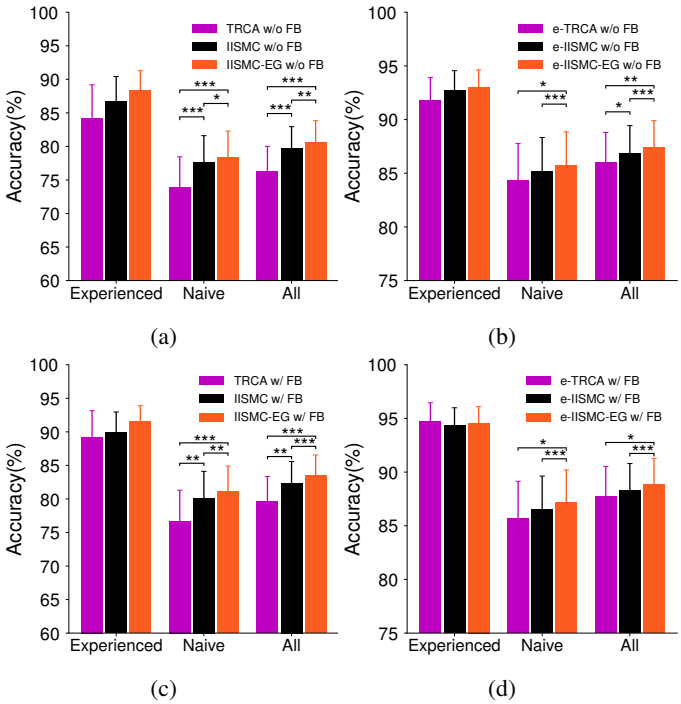

Fig. 7: The average accuracies of three groups (i.e., 8 experienced, 27 naive, and all 35 subjects) obtained by the IISMC-based methods and the TRCA-based methods at a 600ms-long data length. The first and second rows depict the results of these methods without and with the filter-bank (w/o FB and w/ FB) technology, respectively. The asterisk indicates the statistically significant differences (paired t-tests, $*p < 0.05$; $**p < 0.01$; $***p < 0.001$). The error bars indicate standard errors.

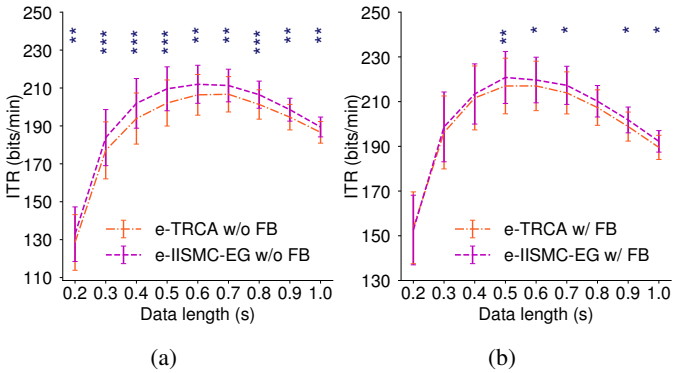

Fig. 8: The averaged ITRs obtained by the ensemble IISMC-based and TRCA-based methods at various time windows without or with filter-bank preprocessing (w/o FB and w/ FB). The ensemble IISMC-based methods selected subjects from the experienced group. The asterisk indicates the statistically significant differences (paired t-tests, $*p < 0.05$; $**p < 0.01$; $***p < 0.001$). The error bars indicate standard errors.

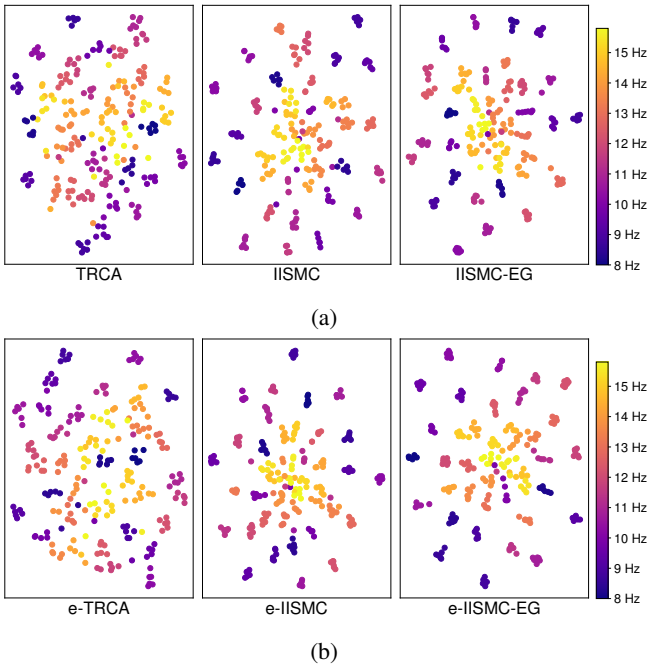

Fig. 9: Two-dimensional t-SNE visualization of the 40-dimensional features obtained by (a) the basic and (b) the ensemble versions of IISMC-based and TRCA-based methods using a 0.6 s time window for an example subject (S22). Each two-dimensional point represents a trial of the 240 total trials and each color represents a stimulation condition.

TRCA, 0.512 for IISMC, 0.553 for IISMC-EG, 0.345 for e-TRCA, 0.557 for e-IISMC, 0.643 for e-IISMC-EG. The average silhouette coefficient of all 35 subjects was also calculated, and the paired t-tests showed significant differences between all pairs of these methods (TRCA: -0.060 $\pm$ 0.048, IISMC: 0.082 $\pm$ 0.049, IISMC-EG: 0.101 $\pm$ 0.049, e-TRCA: 0.000 $\pm$ 0.045, e-IISMC: 0.156 $\pm$ 0.046, e-IISMC-EG: 0.174 $\pm$ 0.046). Therefore, inter-subject similarity and variability can contribute to capturing the inter-subject common features and the inter-class discriminative information.

D. The Computational Time

Fig. 2 showed that the performance of the IISMC was improved as the number of transferred subjects increased. However, such improvement came at the expense of more computational cost. Fig. 10 showed the computational time of the training stage (i.e., calculated the spatial filters and template signals for each frequency) and the prediction stage (i.e., calculated the correlation vectors and output the recognition result) for each method. The evaluation process was carried out on a computer with the configuration of Intel(R) Core(TM) i7-7820X CPU @3.60GHz, 8-core, 64 GB RAM, 64-bit CentOS. The results indicated that the training and prediction time grew linearly with the number of transferred subjects. Meanwhile, the training time accounted for a larger proportion of overall computational time than the prediction time, which inspired us to enable the training stage to run in parallel. Therefore, we assigned one process to each subject involved in the calculation

and then investigated the training time of the parallel IISMC, a parallel version of the IISMC. As shown in Fig. 10(a), data-parallel with multiple processes led to less training time. When there was only one transferred subject, intra- and inter-subject correlation analyses were performed concurrently, resulting in a short training time similar to TRCA's. Although the training time still increased with the number of transferred subjects, a distributed cooperative computing environment could be expected to tackle this problem, which will be investigated in our future work.

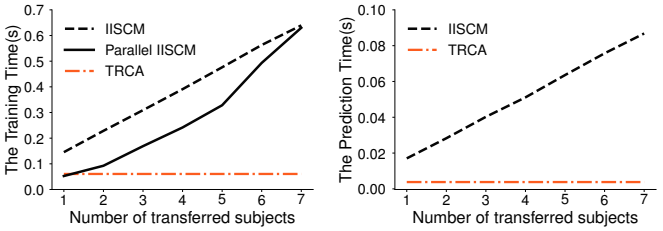

(a) (b)

Fig. 10: The computational time of (a) the training stage and (b) the prediction stage for the IISMC and the TRCA with different number of transferred subjects. In the training stage, the spatial filters and template signals were calculated. In the prediction stage, the correlation vectors were calculated, and the final recognition result was obtained. The data length was set to 0.6 s.

IV. Discussion

A typical BCI system requires time-consuming calibration sessions to collect an adequate amount of labeled individual data. Then, the subject-specific and task-related information is extracted as the features from them [40]. However, the cumbersome calibration procedure restricts the application of SSVEP-based BCIs in the real world. Hence how to reduce training time while maintaining the good BCI performance is one of the main research directions [15]. The previous study, LST [20], developed a cross-subject transferring method to reduce the dependency on the individual calibration data. Similarly, as demonstrated in Fig. 4, when the number of training trials was small, the IISMC-based methods achieved significant improvements in target recognition over the TRCA-based methods. But as the number of training trials increased, the improvements decreased, which emphasizes the importance of individual calibration data for providing subject-specific information [20]. Still, as a whole, the proposed method has the promising potential to reduce dependency on the calibration data as well as shorten the calibration time.

In fact, knowledge transfer between task domains has been proven to be truly beneficial in many cases. In this paper, the IISMC aims to extract the task-related knowledge from several subjects and apply the knowledge to a target subject [41]. Obviously, the experienced group who have experience of using the SSVEP-based BCI speller can provide more useful knowledge and experience. Perhaps the reason is that they can indeed deploy overt attention to the task-relevant stimuli and focus on them [42], which highlights the importance of training in advance. On the other hand, when it is not clear who has the experience, one alternative way is to select subjects with higher accuracy as the ideal transferred subjects (i.e., the experienced group), which has been verified in our previous study [43].

Recently, the collaborative multi-user BCIs have attracted the growing attention of researchers and engineers, which are considered to have potential benefits to improve the overall BCI performance, compared to individual BCIs [44], [45]. In this study, the performance evaluation of the proposed method on the offline dataset suggested that IISMC is a promising cross-subject assistance framework for developing the collaborative BCIs by combining brain signals of multiple subjects who perform the same task. Meanwhile, the cooperative computing architecture will provide optimization for the time consumption of the IISMC algorithm. Therefore, the online collaborative SSVEP-based BCI based on the IISMC method will be investigated in our future work.

V. Conclusion

This study proposed a novel IISMC-based cross-subject assistance framework to enhance the performance of SSVEP-based BCI. Experimental results on 35 subjects showed that the proposed method yielded higher detection accuracies and outperformed the state-of-the-art TRCA method, especially for the IISMC method based on the experienced group. Our experimental results suggested that IISMC has the potential to develop more convenient and practical SSVEP-Based BCI applications.

References

[1] G. Bin, X. Gao, Z. Yan, B. Hong, and S. Gao, "An online multi-channel ssvep-based brain–computer interface using a canonical correlation analysis method," *Journal of neural engineering*, vol. 6, no. 4, p. 046002, 2009.

[2] D. Zhu, J. Bieger, G. Garcia Molina, and R. M. Aarts, "A survey of stimulation methods used in ssvep-based bcis," *Computational intelligence and neuroscience*, vol. 2010, 2010.

[3] X. Chen, Y. Wang, M. Nakanishi, X. Gao, T.-P. Jung, and S. Gao, "High-speed spelling with a noninvasive brain–computer interface," *Proceedings of the national academy of sciences*, vol. 112, no. 44, pp. E6058–E6067, 2015.

[4] Y. Zhang, G. Zhou, J. Jin, M. Wang, X. Wang, and A. Cichocki, "L1-regularized multiway canonical correlation analysis for ssvep-based bci," *IEEE transactions on neural systems and rehabilitation engineering*, vol. 21, no. 6, pp. 887–896, 2013.

[5] Z. Lin, C. Zhang, W. Wu, and X. Gao, "Frequency recognition based on canonical correlation analysis for ssvep-based bcis," *IEEE transactions on biomedical engineering*, vol. 53, no. 12, pp. 2610–2614, 2006.

[6] O. Friman, I. Volosyak, and A. Graser, "Multiple channel detection of steady-state visual evoked potentials for brain-computer interfaces," *IEEE transactions on biomedical engineering*, vol. 54, no. 4, pp. 742–750, 2007.

[7] Y. Zhang, P. Xu, K. Cheng, and D. Yao, "Multivariate synchronization index for frequency recognition of ssvep-based brain–computer interface," *Journal of neuroscience methods*, vol. 221, pp. 32–40, 2014.

[8] G. Bin, X. Gao, Y. Wang, Y. Li, B. Hong, and S. Gao, "A high-speed bci based on code modulation vep," *Journal of neural engineering*, vol. 8, no. 2, p. 025015, 2011.

[9] Y. Zhang, G. Zhou, Q. Zhao, A. Onishi, J. Jin, X. Wang, and A. Cichocki, "Multiway canonical correlation analysis for frequency components recognition in ssvep-based bcis," in *International conference on neural information processing*. Springer, 2011, pp. 287–295.

[10] Y. Zhang, G. Zhou, J. Jin, X. Wang, and A. Cichocki, "Frequency recognition in ssvep-based bci using multiset canonical correlation analysis," *International journal of neural systems*, vol. 24, no. 04, p. 1450013, 2014.

[11] M. Nakanishi, Y. Wang, Y.-T. Wang, and T.-P. Jung, "A comparison study of canonical correlation analysis based methods for detecting steady-state visual evoked potentials," *PloS one*, vol. 10, no. 10, p. e0140703, 2015.

[12] M. Nakanishi, Y. Wang, X. Chen, Y.-T. Wang, X. Gao, and T.-P. Jung, "Enhancing detection of ssveps for a high-speed brain speller using task-related component analysis," *IEEE Transactions on Biomedical Engineering*, vol. 65, no. 1, pp. 104–112, 2017.

[13] Y. Zhang, D. Guo, F. Li, E. Yin, Y. Zhang, P. Li, Q. Zhao, T. Tanaka, D. Yao, and P. Xu, "Correlated component analysis for enhancing the performance of ssvep-based brain-computer interface," *IEEE Transactions on Neural Systems and Rehabilitation Engineering*, vol. 26, no. 5, pp. 948–956, 2018.

[14] K. K. GR and R. Reddy, "Designing a sum of squared correlations framework for enhancing ssvep-based bcis," *IEEE Transactions on Neural Systems and Rehabilitation Engineering*, vol. 27, no. 10, pp. 2044–2050, 2019.

[15] R. Zerafa, T. Camilleri, O. Falzon, and K. P. Camilleri, "To train or not to train? a survey on training of feature extraction methods for ssvep-based bcis," *Journal of Neural Engineering*, vol. 15, no. 5, p. 051001, 2018.

[16] P. Yuan, X. Chen, Y. Wang, X. Gao, and S. Gao, "Enhancing performances of ssvep-based brain–computer interfaces via exploiting inter-subject information," *Journal of neural engineering*, vol. 12, no. 4, p. 046006, 2015.

[17] N. R. Waytowich, J. Faller, J. O. Garcia, J. M. Vettel, and P. Sajda, "Unsupervised adaptive transfer learning for steady-state visual evoked potential brain-computer interfaces," in *2016 IEEE International Conference on Systems, Man, and Cybernetics (SMC)*. IEEE, 2016, pp. 004 135–004 140.

[18] H. Tanaka, "Group task-related component analysis (gtrca): a multivariate method for inter-trial reproducibility and inter-subject similarity maximization for eeg data analysis," *Scientific reports*, vol. 10, no. 1, pp. 1–17, 2020.

[19] M. Nakanishi, Y. Wang, and T.-P. Jung, "Session-to-session transfer in detecting steady-state visual evoked potentials with individual training data," in *International Conference on Augmented Cognition*. Springer, 2016, pp. 253–260.

[20] K.-J. Chiang, C.-S. Wei, M. Nakanishi, and T.-P. Jung, "Cross-subject transfer learning improves the practicality of real-world applications of brain-computer interfaces," in *2019 9th International IEEE/EMBS Conference on Neural Engineering (NER)*. IEEE, 2019, pp. 424–427.

[21] M. M. Müller and S. Hillyard, "Concurrent recording of steady-state and transient event-related potentials as indices of visual-spatial selective attention," *Clinical Neurophysiology*, vol. 111, no. 9, pp. 1544–1552, 2000.

[22] P. Toffanin, R. de Jong, A. Johnson, and S. Martens, "Using frequency tagging to quantify attentional deployment in a visual divided attention task," *International Journal of Psychophysiology*, vol. 72, no. 3, pp. 289–298, 2009.

[23] S. Mun, M.-C. Park, S. Park, and M. Whang, "Ssvep and erp measurement of cognitive fatigue caused by stereoscopic 3d," *Neuroscience letters*, vol. 525, no. 2, pp. 89–94, 2012.

[24] W. Yijun, W. Ruiping, G. Xiaorong, and G. Shangkai, "Brain-computer interface based on the high-frequency steady-state visual evoked potential," in *Proceedings. 2005 First International Conference on Neural Interface and Control, 2005.* IEEE, 2005, pp. 37–39.

[25] S. Saha and M. Baumert, "Intra-and inter-subject variability in eeg-based sensorimotor brain computer interface: a review," *Frontiers in Computational Neuroscience*, vol. 13, p. 87, 2019.

[26] Y. Wang, X. Chen, X. Gao, and S. Gao, "A benchmark dataset for ssvep-based brain–computer interfaces," *IEEE Transactions on Neural Systems and Rehabilitation Engineering*, vol. 25, no. 10, pp. 1746–1752, 2016.

[27] C. S. Herrmann, "Human eeg responses to 1–100 hz flicker: resonance phenomena in visual cortex and their potential correlation to cognitive phenomena," *Experimental brain research*, vol. 137, no. 3-4, pp. 346–353, 2001.

[28] L. C. Parra, S. Haufe, and J. P. Dmochowski, "Correlated components analysis-extracting reliable dimensions in multivariate data," *arXiv preprint arXiv:1801.08881*, 2018.

[29] K. Pearson, "Vii. mathematical contributions to the theory of evolution.—iii. regression, heredity, and panmixia," *Philosophical Transactions of the Royal Society of London. Series A, containing papers of a mathematical or physical character*, no. 187, pp. 253–318, 1896.

[30] J. P. Dmochowski, P. Sajda, J. Dias, and L. C. Parra, "Correlated components of ongoing eeg point to emotionally laden attention–a possible marker of engagement?" *Frontiers in human neuroscience*, vol. 6, p. 112, 2012.

[31] J. P. Dmochowski, M. A. Bezdek, B. P. Abelson, J. S. Johnson, E. H. Schumacher, and L. C. Parra, "Audience preferences are predicted by temporal reliability of neural processing," *Nature communications*, vol. 5, no. 1, pp. 1–9, 2014.

[32] T. G. Dietterich, "Ensemble methods in machine learning," in *International workshop on multiple classifier systems*. Springer, 2000, pp. 1–15.

[33] D. Opitz and R. Maclin, "Popular ensemble methods: An empirical study," *Journal of artificial intelligence research*, vol. 11, pp. 169–198, 1999.

[34] R. Srinivasan, F. A. Bibi, and P. L. Nunez, "Steady-state visual evoked potentials: distributed local sources and wave-like dynamics are sensitive to flicker frequency," *Brain topography*, vol. 18, no. 3, pp. 167–187, 2006.

[35] X. Chen, Y. Wang, S. Gao, T.-P. Jung, and X. Gao, "Filter bank canonical correlation analysis for implementing a high-speed ssvep-based brain–computer interface," *Journal of neural engineering*, vol. 12, no. 4, p. 046008, 2015.

[36] L. v. d. Maaten and G. Hinton, "Visualizing data using t-sne," *Journal of machine learning research*, vol. 9, no. Nov, pp. 2579–2605, 2008.

[37] M. Halkidi, Y. Batistakis, and M. Vazirgiannis, "Clustering validity checking methods: part ii," *ACM Sigmod Record*, vol. 31, no. 3, pp. 19–27, 2002.

[38] P. J. Rousseeuw, "Silhouettes: a graphical aid to the interpretation and validation of cluster analysis," *Journal of computational and applied mathematics*, vol. 20, pp. 53–65, 1987.

[39] J. P. Dmochowski, A. S. Greaves, and A. M. Norcia, "Maximally reliable spatial filtering of steady state visual evoked potentials," *Neuroimage*, vol. 109, pp. 63–72, 2015.

[40] M. Sybeldon, L. Schmit, and M. Akcakaya, "Transfer learning for ssvep electroencephalography based brain–computer interfaces using learn++. nse and mutual information," *Entropy*, vol. 19, no. 1, p. 41, 2017.

[41] S. J. Pan and Q. Yang, "A survey on transfer learning," *IEEE Transactions on knowledge and data engineering*, vol. 22, no. 10, pp. 1345–1359, 2009.

[42] S. Morgan, J. Hansen, and S. Hillyard, "Selective attention to stimulus location modulates the steady-state visual evoked potential," *Proceedings of the National Academy of Sciences*, vol. 93, no. 10, pp. 4770–4774, 1996.

[43] H. Wang, Y. Sun, Y. Li, S. Chen, and W. Zhou, "Inter-and intra-subject template-based multivariate synchronization index using adaptive threshold for ssvep-based bcis," *Frontiers in Neuroscience*, vol. 14, p. 717, 2020.

[44] P. Yuan, Y. Wang, W. Wu, H. Xu, X. Gao, and S. Gao, "Study on an online collaborative bci to accelerate response to visual targets," in *2012 Annual International Conference of the IEEE Engineering in Medicine and Biology Society*. IEEE, 2012, pp. 1736–1739.

[45] P. Yuan, Y. Wang, X. Gao, T.-P. Jung, and S. Gao, "A collaborative brain-computer interface for accelerating human decision making," in *International Conference on Universal Access in Human-Computer Interaction*. Springer, 2013, pp. 672–681.